Annealing of CoFeB/MgO based single and double barrier magnetic tunnel junctions: Tunnel magnetoresistance, bias dependence, and output voltage

G. Feng,[1,a] Sebastiaan van Dijken,[1,b] J. F. Feng,[1] J. M. D. Coey,[1] T. Leo,[2] and David J. Smith[2]
[1]*Department of Physics and CRANN, Trinity College, Dublin 2, Ireland*
[2]*Department of Physics and Astronomy and School of Materials, Arizona State University, Tempe, Arizona 85287, USA*

(Received 2 October 2008; accepted 4 December 2008; published online 11 February 2009)

$Co_{40}Fe_{40}B_{20}$/MgO single and double barrier magnetic tunnel junctions (MTJs) were grown using target-facing-target sputtering for MgO barriers and conventional dc magnetron sputtering for $Co_{40}Fe_{40}B_{20}$ ferromagnetic electrodes. Large tunnel magnetoresistance (TMR) ratios, 230% for single barrier MTJs and 120% for the double barrier MTJs, were obtained after postdeposition annealing in a field of 800 mT. The lower TMR ratio for double barrier MTJs can be attributed to the amorphous nature of the middle $Co_{40}Fe_{40}B_{20}$ free layer, which could not be crystallized during postannealing. A highly asymmetric bias voltage dependence of the TMR can be observed for both single and double barrier MTJs in the as-deposited states and after field annealing at low temperature. The asymmetry decreases with increasing annealing temperature and the bias dependence becomes almost symmetric after annealing at 350 °C. Maximum output voltages of 0.65 and 0.85 V were obtained for both single and double barrier MTJs, respectively, after annealing at 300 °C, a temperature which is high enough for large TMR ratios but insufficient to completely remove asymmetry from the TMR bias dependence. © *2009 American Institute of Physics*. [DOI: 10.1063/1.3068186]

I. INTRODUCTION

Following the first observation of significant tunnel magnetoresistance (TMR) at room temperature,[1,2] magnetic tunnel junctions (MTJs) have emerged as promising components for magnetic sensors and magnetic memory applications. The use of MgO tunnel barriers in these junctions has led to much-enhanced TMR values of several hundred percent at room temperature.[3–8] The combination of good magnetic field sensitivity and large magnetoresistance makes MTJs with MgO barriers suitable for many applications.

The formation of well-crystallized MgO barrier layers is critical in order to obtain high TMR ratios. Molecular beam epitaxy is the most effective way to fabricate MTJs with crystalline barriers. Yuasa *et al.*[3] reported 180% TMR in fully epitaxial Fe (001)/MgO (001)/Fe (001) MTJs. However, it is more convenient to produce highly oriented (001) MgO barriers by sputtering. Parkin *et al.*[4] demonstrated high TMR in MgO based MTJs (up to 220% at room temperature) where a crystalline MgO barrier was prepared using reactive magnetron sputtering. Djayaprawira *et al.*[5] later introduced an alternative way to produce high quality MgO based MTJs. Ferromagnetic layers made from $Co_{40}Fe_{40}B_{20}$ (CoFeB) were deposited by conventional dc sputtering, and the MgO barrier was grown directly by rf sputtering from a MgO target. Remarkably, all of the CoFeB was deposited in an amorphous state, but the MgO grew with a good (001) crystalline texture. Postannealing crystallizes the CoFeB at the MgO interface and produces an oriented stack with crystalline CoFe/MgO interfaces, which is needed to guarantee the large TMR. This is because the MgO only acts a spin filter when it is grown quasiepitaxially between two (001) layers of bcc Fe or CoFe.[9,10]

A significant problem for the application of MTJs is the decrease in TMR with increasing bias voltage across the junction, as it degrades the signal-to-noise ratio. Various explanations for TMR bias dependence have been proposed, including density of state effects in the two magnetic electrodes, spin accumulation effects, or magnon excitation at the metal/barrier interfaces.[11,12] One way to tackle this problem is to fabricate double barrier MTJs (DMTJs), which can be considered as two tunnel junctions connected in series. For equal barriers the applied voltage is evenly divided by the two junctions and the bias on each is halved. This does not improve the maximum TMR of DMTJs, but due to reduced TMR bias dependence the TMR effect is larger at the relevant operation voltage. Although MgO single barrier MTJs (SMTJs) show excellent TMR values, the $V_{1/2}$ voltage, at which the TMR is decreased to half of its maximum value, is still less than 0.80 V.[6] Even for the Fe/MgO/Fe/MgO/Fe DMTJs prepared by molecular beam epitaxy, $V_{1/2}$ is around 1.44 V,[13] which is similar to that of DMTJs with AlO_x barriers.[14–16] In our previous report,[17] we showed that $V_{1/2}$ could be increased up to 1.88 V in MgO based DMTJs.

In this paper we discuss the fabrication of MgO based magnetic tunnel junctions by preparing the crystalline MgO

[a]Electronic mail: fengg@tcd.ie.
[b]Present address: Department of Applied Physics, Helsinki University of Technology, Finland.

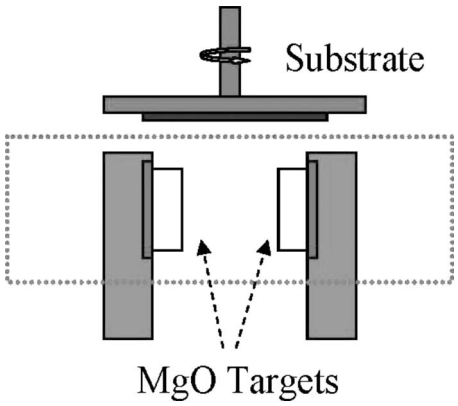

FIG. 1. Schematic illustration of MgO barrier growth using a TFT gun.

barrier with a target-facing-target (TFT) technique, and we investigate the effect of magnetic annealing on tunneling magnetoresistance, bias voltage dependence, and output voltage. The change in the bias dependence of TMR during the magnetic annealing process is explained in terms of the barrier asymmetry. The change of output voltage depends on both TMR ratio and its bias dependence. We show that although the TMR is larger for single MgO barrier, the output voltage is higher for double barrier structures due to the slower decay of the TMR ratio with bias.

II. EXPERIMENT

SMTJs and DMTJs were grown by magnetron sputtering (dc and rf) on thermally-oxidized Si substrates in a Shamrock deposition system with a base pressure of 3×10^{-7} Torr. The system consists of two sputtering chambers. The metallic layers were deposited in the main sputtering chamber and the MgO barrier layer was deposited by rf sputtering from a TFT gun, as illustrated in Fig. 1. In order to establish exchange bias, the wafers were placed in an in-plane magnetic field of 5 mT during the metal deposition. Junctions with sizes varying from 100×100 to 20×20 μm^2 were fabricated using UV lithography and Ar ion-milling techniques. The postdeposition annealing process was performed in a vacuum furnace with an applied magnetic field of 800 mT. The typical temperature ramp-up rate and dwell time were 10 °C/min and 60 min.

A Philips Analytical X-pert Pro x-ray diffractometer with Cu $K\alpha$ radiation was used for structural characterization. The thickness and roughness of MgO single films were obtained by fitting the small angle diffraction patterns. Magnetic properties were measured by alternating gradient force magnetometer (AGFM). The transport properties were characterized by a standard four-point method in an electromagnet system. A positive bias voltage in the transport data corresponds to the situation where electrons tunnel from the top into the bottom electrode. The structure of the MTJ stack was also characterized in cross section by high-resolution transmission electron microscopy (HRTEM) using a JEM-4000EX operated at 400 keV.

III. RESULTS AND DISCUSSION

A. SMTJ and DMTJ stacks

The SMTJ stack used in this study consists of 5 Ta/50 Ru/5 Ta/5 NiFe/10 IrMn/2 CoFe/0.7 Ru/4 CoFeB/2.5 MgO/3 CoFeB/5 Ta/5 Ru (all thicknesses in nanometers). Here, Ta/Ru/Ta serves as a buffer layer, NiFe is a seed layer which induces good (111) texture for IrMn, CoFe is a pinned layer, and the bottom CoFeB electrode is antiferromagnetically coupled to the CoFe through a thin Ru spacer layer in the synthetic antiferromagnetic (SAF) stack. On top of the MgO barrier are the CoFeB free layer and the Ta/Ru capping layer. The DMTJ stack is identical to that of the SMTJ with the addition of another 2.5 MgO/4 CoFeB/0.7 Ru/2 CoFe/10 IrMn/5 NiFe/5 Ta/5 Ru stack on the top of the CoFeB free layer, as shown in Fig. 2(a). All of the layers can be clearly distinguished in the TEM cross-section images [Fig. 2(b)].

The two SAF layers display different exchange biases due to different top and bottom pinning configurations, although the stacks are almost the same. This can be explained by a different degreed texture and grain size for the IrMn

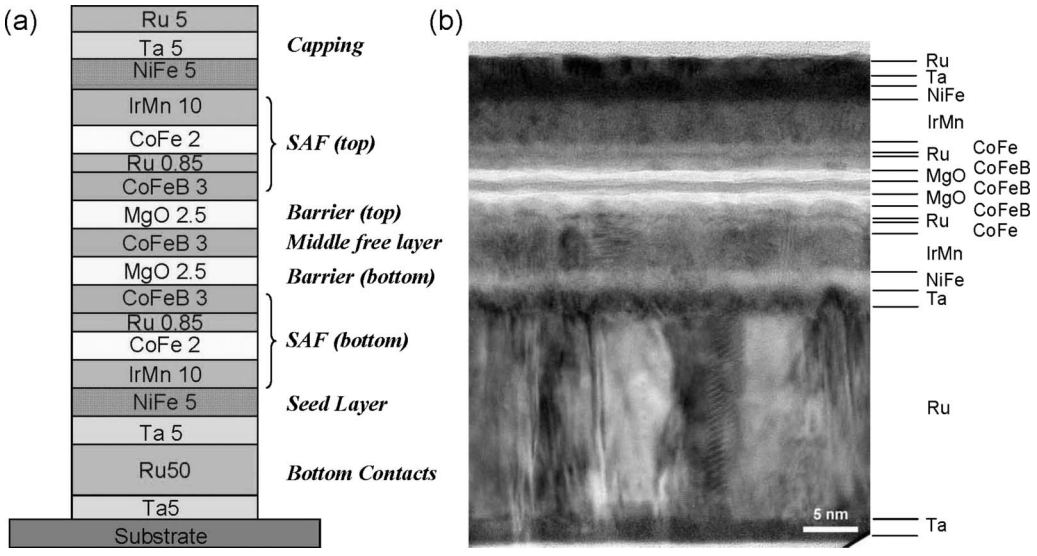

FIG. 2. (a) Stack for the MgO/CoFeB DMTJ and (b) corresponding TEM cross section.

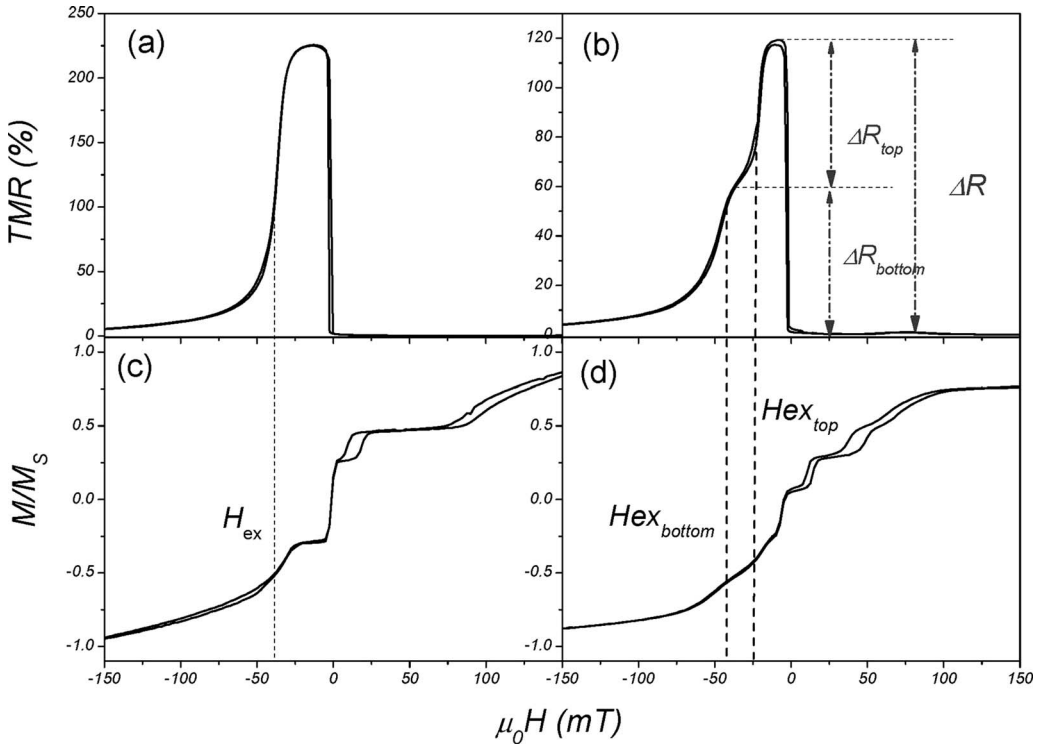

FIG. 3. Room temperature TMR and magnetization curves for [(a) and (c)] SMTJs and [(b) and (d)] DMTJs after annealing at 350 °C for 1 h.

grown on NiFe or CoFe.[18] The same effect on exchange bias was observed in our previous study of spin valves.[19] The middle CoFeB is the free layer, separated from the two pinned layers by 2.5 nm thick MgO barriers. On top of the stack are the Ta capping layers. During microfabrication, another 50 nm layer of Cu was sputtered for the top contact.

B. Annealing effect on TMR

The magnetization and TMR loops for SMTJs and DMTJs after annealing at 350 °C are shown in Fig. 3. From these measurements it is clear that the top and bottom SAF structures exhibit dissimilar exchange bias. As a result, the TMR curve of the DMTJ [Fig. 3(b)] shows a two-step TMR increase at negative applied field, which is different from that of SMTJs [Fig. 3(a)]. The total TMR change during magnetization reversal is a sum of contribution from the bottom and top tunnel barrier junctions, $TMR_{total}=TMR_{bottom}+TMR_{top}$, where TMR_{bottom} and TMR_{top} are the resistance changes in the bottom and top tunnel barriers divided by the total resistance of the DMTJ. The contribution for each SMTJ can be calculated from the TMR curve. In the case of the DMTJ shown in Fig. 3, TMR_{bottom} equals 61% and TMR_{top} equals 58%, so the total TMR is 119% at room temperature. The result suggests that the two barrier layers in our DMTJ device show almost the same resistance. This is good evidence that double tunneling behavior is observed.

The resistance-area (RA) product of a DMTJ for a parallel alignment of the magnetic moment is $5\times10^6\ \Omega\ \mu m^2$, which is about twice the RA product of SMTJs with the same MgO barrier thickness. Together with the equally divided two-step TMR increases, this indicates that electron transport in the DMTJ is characterized by sequential tunneling events and that the DMTJ with 3 nm CoFeB middle free layer can be regarded as two single tunnel junctions that are connected in series.

Figure 4 summarizes the influence of the annealing temperature on the TMR, exchange bias field (H_{ex}), and coercivity of the free layer (H_c) for both SMTJs and DMTJs. With increasing annealing temperature (T_a) up to 375 °C, the TMR increases from a few percent in the as-deposited state to 230% for SMTJs (T_a=375 °C) and 120% for DMTJs (T_a=350 °C). Beyond these annealing temperatures, the TMR begins to drop. The deterioration of the TMR at high annealing temperature is explained by (1) the diffusion of Mn atoms and Ru into the MgO tunnel barrier and (2) the breakdown of exchange bias in the SAF structures.[20,21] The

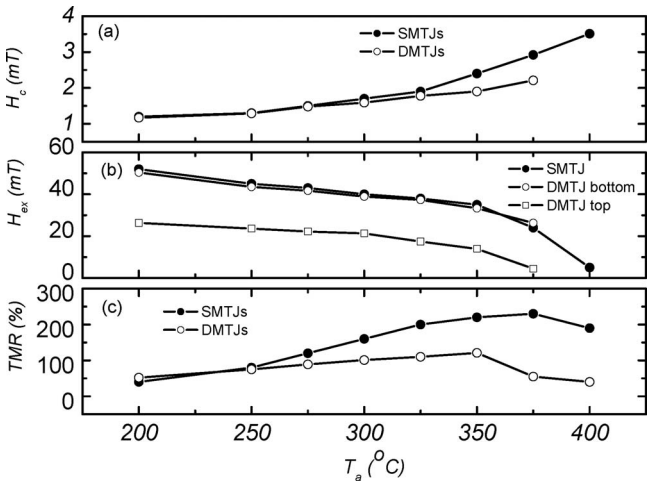

FIG. 4. Annealing temperature dependence of TMR ratio, exchange bias field (H_{ex}), and free layer coercivity (H_c).

latter effect is clearly illustrated by the data of Figs. 4(a) and 4(b), showing an increase in the coercive field and a decrease in exchange bias with increasing annealing temperature. At low T_a, for example, at 200 °C, the annealed SMTJ samples show an exchange bias of 52.2 mT and a coercivity of 1.1 mT. After annealing at 375 °C, although its exchange bias decreases to 23.2 mT and coercivity increases to 3.1 mT, the bottom pinned and top free CoFeB layers still switch independently, following the change of magnetic field. Values of 5.3 and 3.7 mT can be seen for SMTJ samples annealed at 400 °C. The small difference between those two values results in simultaneous magnetization reversal of the pinned and free layers. No perfect antiparallel configuration is obtained in this case.

From those annealing results, we find two notable differences between DMTJs and SMTJs. The first is that the thermal stability of DMTJs is poorer than that of SMTJs. The highest TMR for DMTJs is achieved at 350 °C and begins to drop after annealing at 375 °C for 1 h, although this is the best annealing temperature for SMTJs in terms of getting high TMR. This result can be understood by taking account of the top SAF structure used in the DMTJ stacks. The exchange bias of the top SAF becomes already negligibly small after annealing at T_a=350 °C. Subsequent increase in coercive field of the middle free layer at higher annealing temperature further reduces the TMR of DMTJs. After annealing at 400 °C, a 40% TMR can be still obtained from the field versus resistance curve for the DMTJ samples but switches between the free layer and the top pinned layer are unseparated. The top pinned layer totally loses its exchange bias. This is the reason why the exchange bias field (H_{ex}) and coercivity of the free layer (H_c) for the DMTJ annealed at 400 °C are not included in Figs. 4(a) and 4(b). The poorer thermal stability of the top SAF structure is most likely due to a lower onset temperature for Mn diffusion from the top IrMn layer towards the MgO/CoFeB interface.[22]

Besides the difference in the evolution of the TMR with annealing temperature, the maximum TMR (TMR_{max}) is also considerably larger for SMTJs as compared to DMTJs with the same bottom electrode and free layer structure. TMR_{max} is around 230% for SMTJs, which is almost twice the value for DMTJs (120%). It is not obvious why this is the case as sequential tunneling is expected to yield the same TMR when the thickness and quality of the ferromagnetic layers and tunnel barriers are identical. The lower TMR_{max} ratio observed, therefore, indicates that there must be some difference in the magnetic and barrier layers of the DMTJs and SMTJs.

In order to investigate the different annealing behavior, high-resolution transmission electron micrographs have been recorded close to the double MgO barriers. Figure 5 shows electron micrographs of the MgO double barrier structure in the as-deposited state and after annealing at 350 °C. The thicknesses for the CoFeB and MgO are around 3.0 and 2.5 nm, as expected. The MgO layers exhibit a (001) texture after deposition and this does not improve much upon annealing. The wavy bottom surface of the bottom tunnel barrier reflects the morphology of the underlying Ta/Ru/Ta/NiFe/IrMn stack. All three CoFeB layers are observed to be

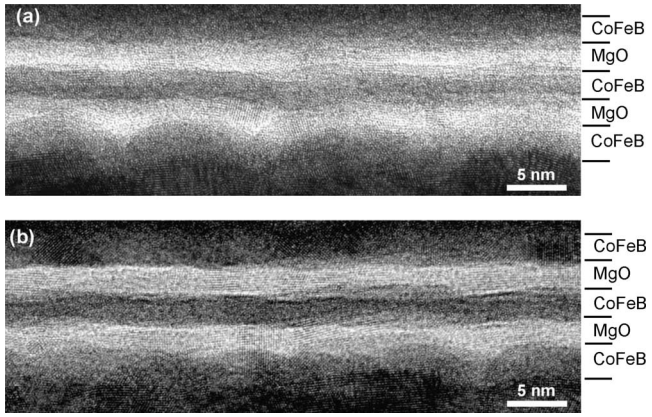

FIG. 5. Electron micrographs from the barrier region of DMTJs (a) as deposited and (b) after annealing at 350 °C.

amorphous in the as-deposited state. The annealing process crystallizes the bottom and top CoFeB electrodes, but there is no sign of any crystallinity in the middle CoFeB layer. As a high degree of film texture in the ferromagnetic electrodes and MgO (001) barrier is a prerequisite for large TMR ratios,[9,10] the amorphous nature of the free layer in the DMTJs explains its smaller TMR.

It is interesting to compare these results for DMTJ with studies of crystallization for single CoFeB layers or in MgO based SMTJs. For example, it has been suggested that the MgO barrier acts as a boron sink which promotes the crystallization of CoFeB during annealing.[7,23–25] In our case, since the middle CoFeB remains amorphous, it appears that the MgO layers on either side of the middle CoFeB layer must act as barriers to boron diffusion. The free layer is unlike the other two CoFeB pinned layers, where boron can also diffuse into adjacent metallic layers. This situation is unresolved and a nanoscale boron profile is needed before any definitive conclusions can be drawn. Another possibility is that the adjacent Ru layers can initiate the crystallization of two amorphous CoFeB pinned layers during annealing.[26–28] One other factor which would influence the crystallinity of the CoFeB free layer is a lack of coherence of the crystal structures of the two adjacent MgO layers. While both have a (001) texture, they grow independently on amorphous CoFeB, which would make it difficult for the middle free layer to crystallize quasiepitaxially on both of them.

C. Annealing effect on the bias dependence of TMR

One of the advantages of DMTJs for practical application is a slower decay of the TMR with bias voltage. Figure 6 compares the TMR bias dependence of DMTJs and SMTJs, which share the same bottom electrode and barrier thickness after annealing at 300 °C. The normalized TMR versus bias voltage curves are asymmetrical in both cases, and the TMR drops much faster in the negative bias branch. This asymmetry may have been caused by differences in the electronic states of the upper and lower MgO/CoFeB interfaces. In the case of DMTJs, this asymmetry is more obvious compared with SMTJs. It is understood that the addition of interfaces in the DMTJs brings more differences than in the

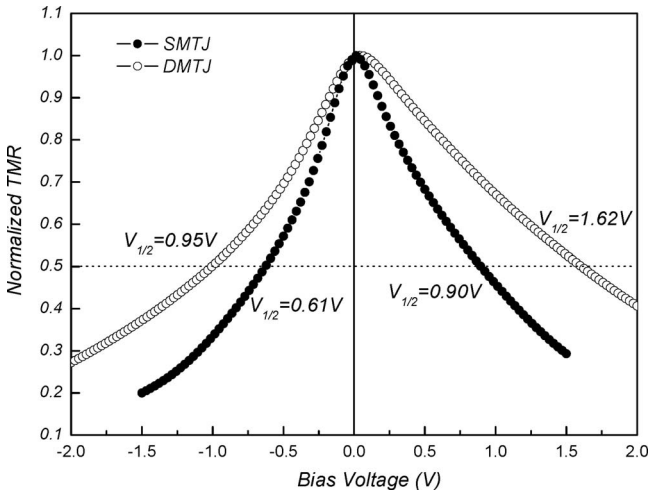

FIG. 6. Normalized room temperature TMR as a function of bias voltage for a SMTJ and a DMTJ after annealing at 325 °C.

SMTJs. The $V_{1/2}$ bias voltages are −0.97 and 1.62 V for the DMTJ, which are considerably larger than −0.61 and 0.90 V measured on the SMTJ. The maximum $V_{1/2}$ values for the DMTJ in the positive part are also higher compared with those of Fe/MgO DMTJs (Ref. 13) and CoFeB/AlO_x.[14,15]

The TMR bias voltage dependence of DMTJs after annealing at different temperatures is summarized in Figs. 7(a) and 7(b). Annealing at a low temperature of 200 °C results in values of $V_{1/2}^{+}=1.88$ V and $V_{1/2}^{-}=-0.94$ V. This large bias asymmetry reflects the dissimilar CoFeB/MgO interfaces in moderately annealed DMTJ stacks. Annealing DMTJs at 350 °C, on the other hand, almost completely removes the bias asymmetry. In that case, $V_{1/2}^{+}=1.10$ V and $V_{1/2}^{-}=-1.17$ V. In addition, an increase in the annealing temperature shifts the maximum of the TMR curve toward zero bias, which can be seen from Fig. 7(b). This shift (Δ_{shift}), which can be as large as 120 mV for samples that are annealed at 200 °C, reduces to only 16 mV when an annealing temperature of 350 °C is used. The offset in the TMR curves reflects an initially larger increase in the tunneling conductance with positive applied bias for parallel rather than antiparallel aligned magnetic moments.

The variation in the TMR ratio with annealing temperature and bias voltage is qualitatively similar for SMTJs. Figure 8 summarizes the annealing temperature effects on $V_{1/2}^{+}$, $V_{1/2}^{-}$, $\Delta V_{1/2}=|V_{1/2}^{+}-V_{1/2}^{-}|$ and shift in the bias voltage dependence of the TMR (Δ_{shift}) for both MTJs. With increasing annealing temperature, $V_{1/2}^{-}$ increases and $V_{1/2}^{+}$ decreases. These values for DMTJs [Fig. 8(b)] are much larger than for the SMTJs [Fig. 8(a)], and the fact that the SMTJ exhibits small asymmetry with respect to the DMTJ suggests that the two MgO tunnel barriers in the DMTJ have similar TMR versus bias voltage dependencies.

The bias shift of maximum TMR (V_{bias}) has also been reported in single barrier AlO_x-based MTJs, and it is explained in two different ways. Sato *et al.*[29] considered Co–Al interdiffusion and a change in band structure after annealing as a possible cause for the shift; Oepts *et al.*[30] believed that the barrier asymmetry ($\Delta\phi$) can be the reason for the shift of maximum TMR versus bias curve. The calculations of the latter group clearly showed the change from asymmetric to symmetric bias with decreasing $\Delta\phi$. They also assumed that the change of the barrier height ($\Delta\phi$) was related to oxidation time in the preparation of the AlO_x barrier.

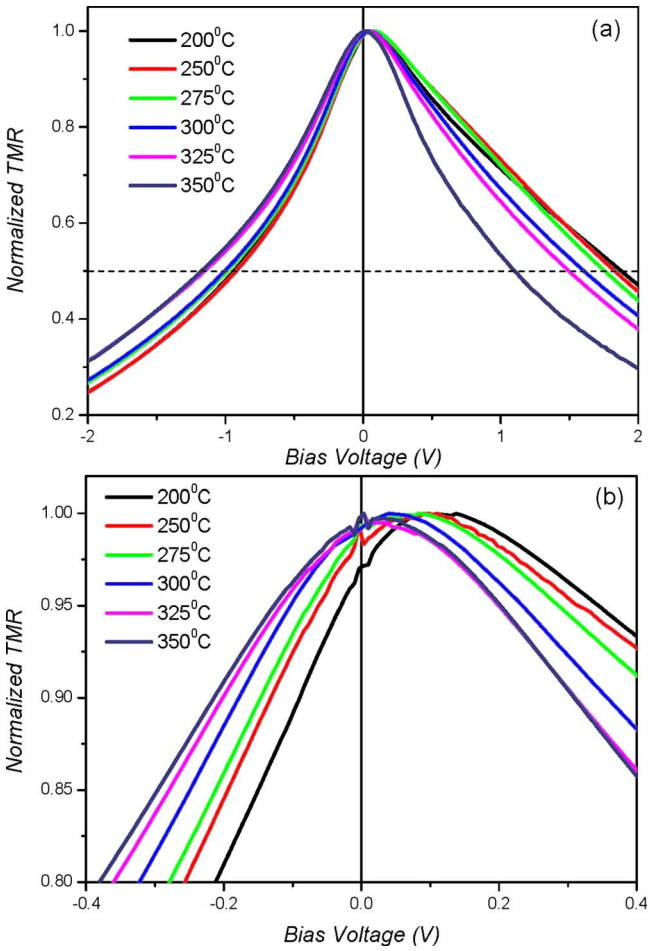

FIG. 7. (Color online) (a) Normalized TMR vs bias voltage curves for DMTJs annealed at different temperatures and (b) a close-up clearly showing a shift of the curve away from zero bias for low annealing temperatures.

Figure 9 schematically illustrates the influence of an asymmetry tunnel barrier on the bias voltage dependence of the TMR. Of course, the results should be interpreted only as an indication of the effect of the asymmetry of the potential barrier on asymmetry of the TMR versus bias voltage in our MgO based MTJs. The changing of the bias dependence curves with decreasing $\Delta\phi$ is very similar to its evolution with increasing annealing temperature. So it is reasonable to speculate that the shift of maximum TMR (V_{bias}) could be a result of the change of $\Delta\phi$ during annealing. For the MgO based SMTJs and DMTJs, the tunnel barrier asymmetry is most likely due to variations in the degree of film texture in the MgO and CoFeB layers, which is drastically reduced upon annealing at elevated temperatures. A large difference of barrier height between the bottom and top electrodes ($\Delta\phi$) for as-deposited or low-temperature annealed samples will result in a shift of the maximum TMR (V_{bias}) to positive bias. With increasing annealing temperature ($T_1 > T_2 > T_3$ as indicated in Fig. 9), $\Delta\phi$ decreases. The maximum TMR (V_{bias}) will shift to zero bias as the bias dependence curves become more symmetric.

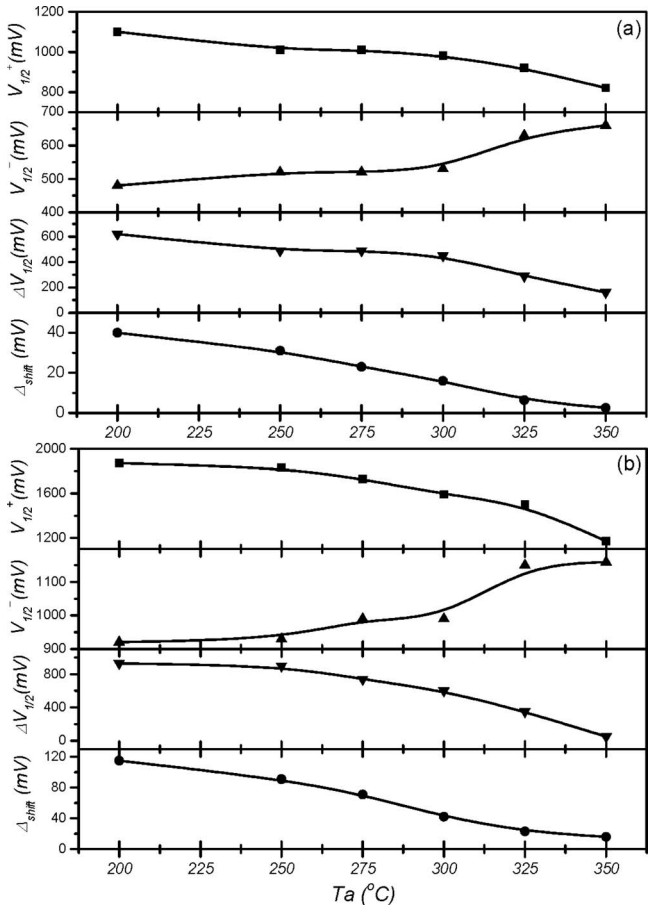

FIG. 8. $V_{1/2}^{+}$, $V_{1/2}^{-}$, $\Delta V_{1/2}$, and Δ_{shift} for (a) SMTJ and (b) DMTJ structures as functions of annealing temperature.

D. Annealing effect on output voltage

For sensor and memory applications, the variation in the MTJ output voltage, $V_{\text{out}}=V\times(R_{\text{AP}}-R_{\text{P}})/R_{\text{AP}}$, is an important parameter. Figure 10 summarizes the output voltage as a function of annealing temperature for DMTJs and SMTJs. From these curves the two maximum output voltages, $V_{\text{out,max}}$, under positive and negative biases, can be obtained. $V_{\text{out,max}}$ is 0.56 V for the SMTJ and increases to 0.85 V for the DMTJ for the positive bias branch, and it is 0.41 and 0.68 V for the negative branch. Although DMTJs show lower TMR compared with SMTJs, the remarkable improvement of bias dependence can still result in a higher $V_{\text{out,max}}$. As pointed out previously, the TMR shows the maximum at 375 and 350 °C for SMTJs and DMTJs, respectively. However, unlike TMR, the $V_{\text{out,max}}$ under positive bias for both DMTJ and SMTJ is obtained after annealing at 300 °C. This difference is due to a slow decay of the $(R_{\text{AP}}-R_{\text{P}})/R_{\text{AP}}$ ratio with positive bias voltage at low annealing temperatures. Under negative bias, the $(R_{\text{AP}}-R_{\text{P}})/R_{\text{AP}}$ ratio always improves with increasing annealing temperature, so that $V_{\text{out,max}}$ reaches its maximum after high temperature annealing.

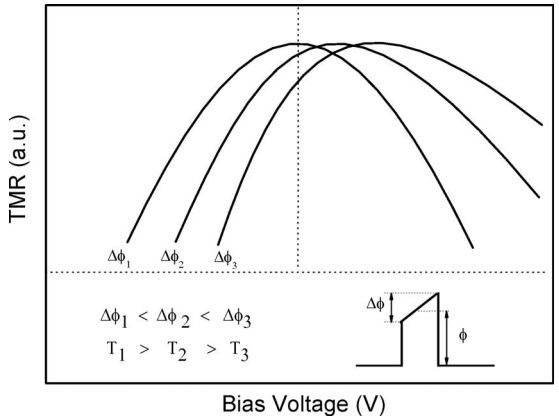

FIG. 9. Schematic illustration of the influence $\Delta\phi$ on the asymmetry in TMR vs bias voltage curves [based on the calculations of Oepts *et al.* (Ref. 30)].

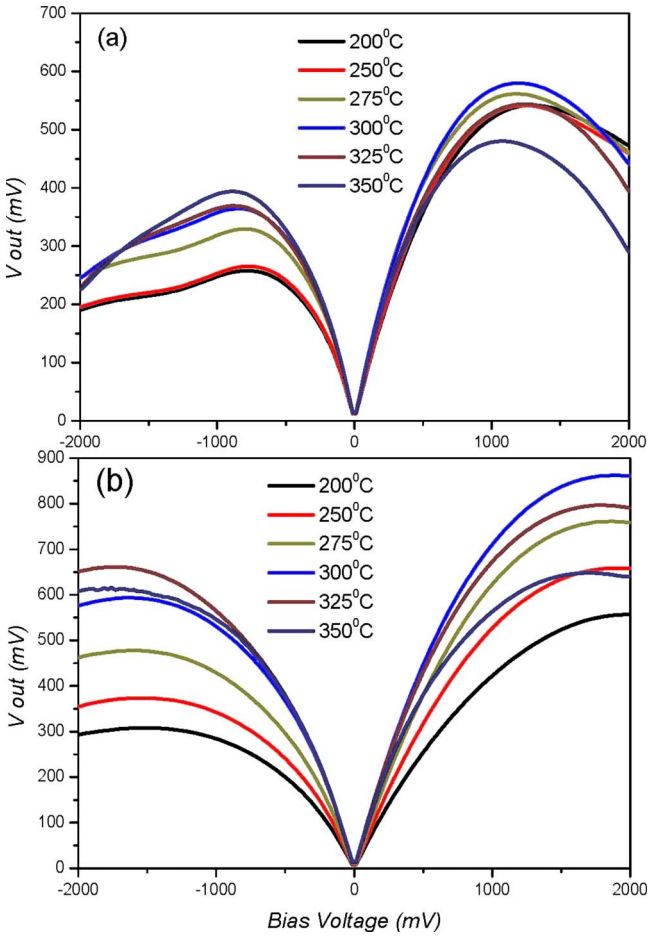

FIG. 10. (Color online) (a) DMTJ and (b) SMTJ output voltages as functions of applied bias after annealing at different temperatures.

The magnitude of the maximum output voltage of our DMTJ is larger than those reported for fully epitaxial Fe/MgO/Fe (Ref. 3) and CoFeB/MgO/CoFeB SMTJs.[5,6] The data in Fig. 10 clearly show that a maximum output signal is obtained after annealing at a temperature at which the asymmetry in the bias voltage dependence on the TMR is still significant and the TMR ratio is relatively high. This feature can be used to optimize the output voltage of MTJs in practical applications.

IV. CONCLUSIONS

We have successfully fabricated single and double barrier MgO MTJs with CoFeB electrodes exhibiting large room temperature TMR of 230% and 120%, respectively. Clearly

separated magnetization switches for top and bottom SAF layers and an improved bias dependence have been realized in the double MTJs. The magnetic thermal annealing enhances the TMR ratio for both MTJs but the double barrier shows a lower TMR ratio compared with the single barrier. Electron micrograph revealed that the middle CoFeB free layer cannot be crystallized even after high temperature annealing, and this is thought to be the main reason for the lower TMR in the DMTJs. Further improvement of the DMTJs may require a better crystallographic coherence in the multilayer stacks so that the middle CoFeB free layer can crystallize at the same time as the top and bottom electrodes. Despite the lower TMR ratio, the double barrier junctions exhibit a larger output voltage than SMTJs. This is due to a slower decay of the TMR ratio with bias voltage in DMTJs and is further enhanced by a large MgO tunnel barrier asymmetry after annealing at moderate temperatures.

ACKNOWLEDGMENTS

This work was supported by Science Foundation Ireland as part of the CINSE and MANSE projects, and European BIOMAGSENS project. We are grateful to H. C. Wu for the AGFM measurement.

[1]J. S. Moodera, L. R. Kinder, T. M. Wang, and R. Merservey, Phys. Rev. Lett. **74**, 3273 (1995).
[2]T. Miyazaki and N. Tezuka, J. Magn. Magn. Mater. **139**, L231 (1995).
[3]S. Yuasa, T. Nagahama, A. Fukushima, Y. Suzuki, and K. Ando, Nature Mater. **3**, 868 (2004).
[4]S. S. P. Parkin, C. Kaiser, A. Panchula, P. M. Rice, B. Hughes, M. Samant, and S.-H. Yang, Nature Mater. **3**, 862 (2004).
[5]D. D. Djayaprawira, K. Tsunekawa, M. Nagai, H. Maehara, S. Yuasa, Y. Suzuki, and K. Ando, Appl. Phys. Lett. **86**, 092502 (2005).
[6]J. Hayakawa, S. Ikeda, F. Matsukura, H. Takahashi, and H. Ohno, Jpn. J. Appl. Phys., Part 2 **44**, L587 (2005).
[7]Y. M. Lee, J. Hayakawa, S. Ikeda, F. Matsukura, and H. Ohno, Appl. Phys. Lett. **90**, 212507 (2007).
[8]S. Ikeda, J. Hayakawa, Y. Ashizawa, Y. M. Lee, K. Miura, H. Hasegawa, M. Tsunoda, F. Matsukura, and H. Ohno, Appl. Phys. Lett. **93**, 082508 (2008).
[9]W. H. Butler, X.-G. Zhang, T. C. Schulthess, and J. M. MacLaren, Phys. Rev. B **63**, 054416 (2001).
[10]J. Mathon and A. Umerski, Phys. Rev. B **63**, 220403 (2001).
[11]S. Zhang, P. M. Levy, A. C. Marley, and S. S. P. Parkin, Phys. Rev. Lett. **79**, 3744 (1997).
[12]C. Lu, M. W. Wu, and X. F. Han, Phys. Lett. A **319**, 205 (2003).
[13]T. Nozaki, A. Hirohata, N. Tezuka, S. Sugimoto, and K. Inomata, Appl. Phys. Lett. **86**, 082501 (2005).
[14]K. Nakajima, Y. Saito, S. Nakamura, and K. Inomata, IEEE Trans. Magn. **36**, 2806 (2000).
[15]S. Colis, G. Gieres, L. Bar, and J. Wecker, Appl. Phys. Lett. **83**, 948 (2003).
[16]Z. M. Zeng, H. X. Wei, L. X. Jiang, G. X. Du, W. S. Zhan, and X. F. Han, J. Magn. Magn. Mater. **303**, e219 (2006).
[17]G. Feng, S. van Dijken, and J. M. D. Coey, Appl. Phys. Lett. **89**, 162501 (2006).
[18]H. N. Fuke, K. Saito, M. Yoshikawa, H. Iwasaki, and M. Sahashi, Appl. Phys. Lett. **75**, 3680 (1999).
[19]E. Kerr, S. van Dijken, and J. M. D. Coey, J. Appl. Phys. **97**, 093910 (2005).
[20]J. Hayakawa, S. Ikeda, Y. M. Lee, F. Matsukura, and H. Ohno, Appl. Phys. Lett. **89**, 232510 (2006).
[21]X. Y. Liu, D. Mazumdar, W. F. Shen, B. D. Schrag, and G. Xiao, Appl. Phys. Lett. **89**, 023504 (2006).
[22]Y. K. Kim, G. H. Park, S. R. Lee, S. H. Min, J. Y. Won, and S. A. Song, J. Appl. Phys. **93**, 7924 (2003).
[23]D .J. Kim, J. Y. Bae, W. C. Lim, K. W. Kim, and T. D. Lee, J. Appl. Phys. **101**, 09B505 (2007).
[24]J. Y. Bae, W. C. Lim, H. J. Kim, T. D. Lee, K. W. Kim, and T. W. Kim, J. Appl. Phys. **99**, 08T316 (2006).
[25]T. Takeuchi, K. Tsunekawa, Y. S. Choi, Y. Nagamine, D. D. Djayaprawira, A. Genseki, Y. Hoshi, and Y. Kitamoto, Jpn. J. Appl. Phys., Part 2 **46**, L623 (2007).
[26]C. Park, J.G. Zhu, M. T. Moneck, Y. Peng, and D. E. Laughlin, J. Appl. Phys. **99**, 08A901 (2006).
[27]C. Park, Y. H. Wang, D. E. Laughlin, and J. G. Zhu, IEEE Trans. Magn. **42**, 2639 (2006).
[28]Y. H. Wang, W. C. Chen, S. Y. Yang, K. H. Shen, C. Park, M. J. Kao, and M. J. Tsai, J. Appl. Phys. **99**, 08M307 (2006).
[29]M. Sato, H. Kikuchi, and K. Kobayashi, IEEE Trans. Magn. **35**, 2946 (1999).
[30]W. Oepts, M. F. Gillies, R. Coehoorn, R. J. M. van de Veerdonk, and W. J. M. de Jonge, J. Appl. Phys. **89**, 8038 (2001).